Available online at www.sciencedirect.com

ScienceDirect

Procedia Materials Science 4 (2014) 221 – 226

Procedia Materials Science

www.elsevier.com/locate/procedia

8th International Conference on Porous Metals and Metallic Foams, Metfoam 2013

Modelling stochastic foam geometries for FE simulations using 3D Voronoi cells

P. Siegkas[a,*], V. Tagarielli[b], N. Petrinic[a]

[a]*Department of Engineering Science, University of Oxford, Pegbroke Science Park, I.E.L., Oxford OX51PF, UK*
[b]*Department of Aeronautics, Imperial College London, South Kensington Campus, London SW72AZ, UK*

Abstract

A method for generating realistic foam geometries is developed for modelling the structure of stochastic foams. The method employs 3D Voronoi cells as pores. The virtual geometries are subjected to loading with the use of finite element methods and the results are compared to experimental data for open cell Titanium foams. The method applies statistical control to geometrical characteristics and it's used to either replicate or virtually generate prototype foam structures.

Peer-review under responsibility of Scientific Committee of North Carolina State University

Keywords: Finite Element; Microscale; Modelling; Titanium Foam; Voronoi Simulation.

1. Introduction

Various authors have investigated cellular materials for use in medical implants (Eppley and Sadove (1990), Karageorgiou and Kaplan (2005), Navarro et al. (2008), Khanoki and Pasini (2012)). Methods such as powder sintering in combination with space holder techniques are often used to produce metallic foams tailored to mechanical requirements of porous bone substitutes (Niu (2009), Davies and Zhen (1983)). The produced cellular structures are commonly characterised experimentally to provide information towards optimisation and ensure compliance to requirements (Oh et al. (2003), Imwinkelried (2007), Li et Al. (2008), Siegkas et al. (2011)).

* Corresponding author. Tel.: +44-186-561-3452; fax: +44-18-652-73906.
E-mail address: petros.siegkas@eng.ox.ac.uk

Peer-review under responsibility of Scientific Committee of North Carolina State University
doi:10.1016/j.mspro.2014.07.604

The geometries of open cell irregular foams are usually complex and difficult to create or replicate for finite element analysis. Some commercial software packages are able to reproduce foam geometries using x-ray micro tomography (XMT) scans (Sitek et al. (2006)) but these are usually expensive and tomography equipment is not always accessible. This study is focused in virtually generating realistic foam geometries with desirable microstructural characteristics. Shen et al (Shen et al. (2006)), simulated structures of foams based on a method of growth of pressurised pores. Pores were represented by spheres that grew to achieve desirable density for foams up to 15 % of porosity. Borovinsek, et al (Borovinšek and Ren (2008)), modelled high porosity lattice structures 88-97 % based on the Voronoi tessellations. The study was purely numerical. Singh et al (Singh et al. (2010)), tested Ti foams of porosities of 51-78 % and modelled the structure using FE methods. The geometry of the foam was obtained using X-ray micro tomography from which the structure was reconstructed and directly meshed (5000000 elements) using commercial software. The used methods and software were considerably expensive and FE predictions diverged up to 40 % from the experiments.

This work is focused in developing a method for capturing and investigating the microstructural characteristics that affect the macroscopic response in highly irregular foams. The process in this study provides with a tool for replicating and potentially tailoring foams to the constraints of applications.

2. Methods and models

The pores of highly irregular foams form complex networks of random shapes and texture. Voronoi polyhedrals are suitable for replicating these random structural characteristics by using them either individually or in clusters of Voronoi cells. The Voronoi tessellation is a method by which a space is separated in cells (Voronoi (1908)). Every point in the periphery of the cells is closer to its seed point than to any other. In 3D the Voronoi tessellations produce polyhedrals. Their size and shape depends on the amount and position of the initial seed points.

The microstructure of the foams was generated using random 3D Voronoi tessellations. The Voronoi polyhedrals were randomly placed within a cube. The cavity in-between the polyhedrals and the boundary of the cube were meshed and then the polyhedrals were deleted creating a network of pores (Fig. 1).

The foam structure produced by this method is defined as follows:

A number of bounded X_i volumes (Voronoi cells), form a set called X where $X=(\cup X_i)$ and X_1, X_2, X_3 … $X_n \subseteq R^3$. The set X: is bounded by an external surface V_B that contains a volume V_B where $X_i \subseteq V B \forall_i$. The Foam space Y is defined by Eq. 1 and demonstrated in Fig. 1.

$$Y = V_B - (\cup X_i) \text{ where } Y, V_B \subseteq R^3 \quad (1)$$

The foam's type (open or closed cell), inner structure and texture, can be changed by altering characteristics and criteria of the set X (of Voronoi polyhedrals) (Figs.2 and 3).

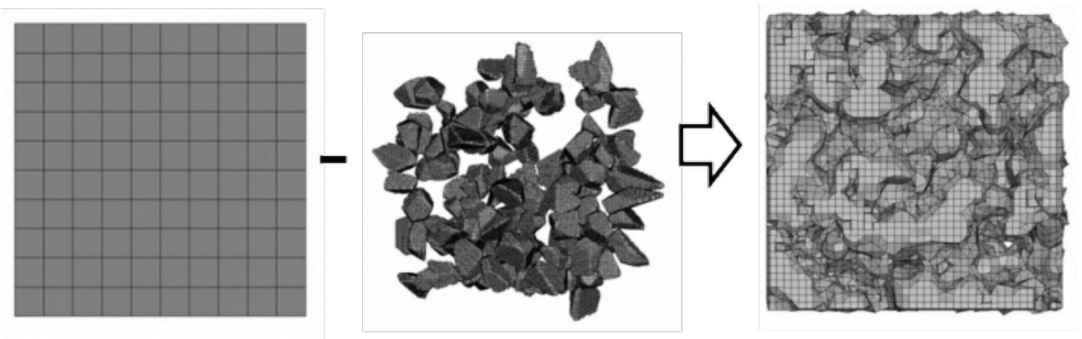

Fig. 1. Graphic representation of the stochastic geometry generation. The randomly shaped Voronoi polyhedrals are used to form the pore network. The cavity in-between the polyhedrals (set of pores) and the boundary of the cube is meshed and the polyhedrals are deleted creating a network of pores.

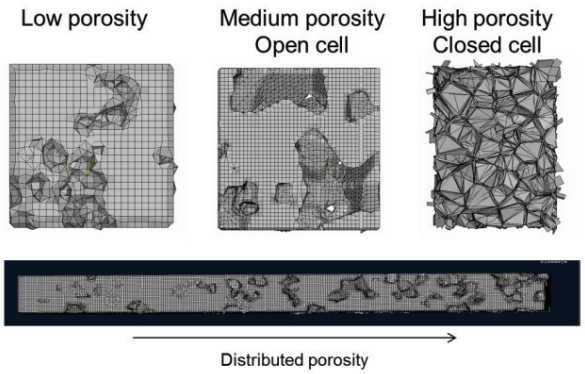

Fig. 2. Geometries produced using Voronoi cells. Changing the statistical characteristics of the seed points and number of pores, results in different types of foam.

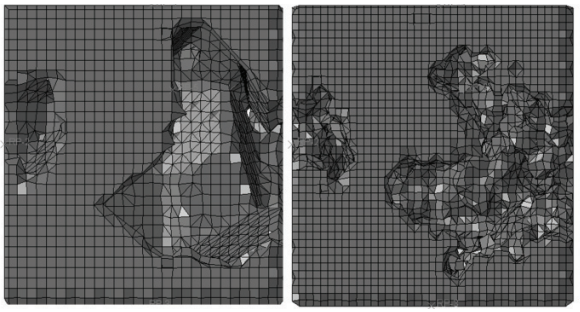

Fig. 3. Comparison of a foam structures with smooth (left) and rough (right) cell walls. Clusters of Voronoi cells can form pores or material to replicate the texture of the sintered powders.

For each virtual specimen a set of pores was produced to form the structure. The size distribution of the set was based on XMT scans performed on this type of foams (Siegkas et al. (2011)). The volume ratio between the pore set and the specimen would give the macroporosity. The volume of the pore set (Voronoi polyhedrals) was kept constant and porosity was regulated by altering the size of the specimen. The representative volume element for the geometrical characteristics was defined as the volume that can enclose the set of pores and produce the desirable ratio of pore to specimen volume. The size of the surrounding cubic frame was defined based on the needed cube volume V_{B} that would produce the targeted pore to specimen ratio (porosity).

The average polyhedral size was controlled by the number of points within the cube (Eq. 2). The polyhedral sizes followed the target pore size distribution (Siegkas et al. (2011)). The distribution curve was discretised to 4 intervals. For each interval of the pore size distribution a number of points was randomly placed within the estimated cube volume.

The number of points was calculated using (Eq. 2) to achieve the desirable pore size. The volume was then separated to Voronoi polyhedral and a number of cells corresponding to the distribution was flagged as pores. A proximity criterion was applied in choosing suitable pores so that pores of different size intervals would not completely overlap. The criterion was defined by considering a distance around the seed points that corresponded to the equivalent radius of a sphere of the same volume as the average polyhedral cell. Due to the irregular shape of the cells the criterion can allow for some overlapping therefore creating open cell structures.

$$\overline{V}_{\mathrm{p}} = \frac{V_{\mathrm{B}}}{i} \tag{2}$$

Where $\overline{V}_P$ is the average pore size, V_B is the specimen volume size, i is the number of seed points. The volume of the virtual specimen V_B is defined based on the targeted total porosity. The experimentally examined foams (Siegkas et al. (2011)) had two types of porosity. Macro-pores corresponding to the distribution were of the order of 100 μm and micro-pores of the order of 10 μm at a percentage of 10 % within the parent material. The parent material was

formed by sintered Ti powders and was tested without macro pores in order to study its properties (Siegkas et al. (2011)). The Voronoi polyhedrals were used to generate the macroporosity and the parent material was represented as a pseudo-continuum with corresponding density. The percentage of micro-porosity corresponding to the parent material was included in calculations to determine the total porosity (Eq. 3) and the volume of each virtual specimen (Eqs. 4 and 5). The total porosity for the virtual specimens was chosen to either replicate existing foam specimens or virtually generate densities of the same type.

The volume of macro-pores was given by the distribution (Siegkas et al. (2011)). Macro-porosity (volume ratio) was calculated through (Eqs. 3 and 4). The volume of the cubic specimen V_B was then defined by solving (eq. 5) in respect to V_B. An iterative process was followed to achieve good match of target porosity and the porosity of the generated foam. The irregularity of the polyhedral cells results to some porosity loss that causes divergence between the final porosity from the originally targeted. The loss is mainly due to the partial overlapping amongst the pores and between pores and specimen boundary. Partial overlapping is necessary for creating the open cell structure. An average correction factor (c) was taken into account (Eq. 5) for iteratively defining the specimen volume V_B. For the first attempt, Eq. 5 would be solved in respect to V_B considering c equal to zero. The factor (c) would then be determined as the difference of targeted macroporosity P_M and the actually achieved porosity. Based on the new (c) Eq. 5 would be solved again in respect to V_B so that to adjust the volume to the geometry irregularity and partial pore overlapping.

$$\mathrm{P_t} = \mathrm{P_M} + \mathrm{P_m} \tag{3}$$

$$\mathrm{P_m} = 0.1(1 - \mathrm{P_M}) \tag{4}$$

$$\mathrm{P_M} = \frac{1}{V_\mathrm{B}} P_\mathrm{N} \sum_{1}^{\mathrm{n}} A_\mathrm{n} V_\mathrm{n} - \mathrm{c} \tag{5}$$

Where: P_t is the total porosity, P_M is porosity due to macro-pores, P_m is porosity due to micro-pores, A_n is the probability of each pore size from the distribution curve, P_N is the number of all macro-pores (pore set), V_n is average size of each of the size intervals, V_B is volume of specimen, n is the number of size intervals from the distribution, c is a correction factor related to the irregularity of pores and degree of overlapping (c is defined through an iterative process).

The cavity between the cube and the Voronoi cells was meshed by commercial software (Ansa (2007)) using linear elements.

The Voronoi cells on the boundary of the cubic space would often have sharp edges and extend their boundaries outside the cube. The quality of the Voronoi cells was improved by tessellating a larger cubic space than needed and only using cells from the interior core rather than the boundary

A combination of developed code and commercial software was used to produce the foam mesh. The Voronoi polyhedrals were produced using code developed in Matlab (Mathworks (2002)) that would export a shell mesh in (.key) LS Dyna format (L. S. T. Corporation (2007)). The confining shell cube would then be produced in LS Dyna-prepost software and then imported in commercial meshing software (Ansa Beta CAE) (Ansa (2007)) where it would be meshed as a solid and exported for FE software (Dassault Systèmes Simulia Corp. (2009)) Fig.4. The produced meshes would have between 38000-83000 nodes.

The meshed specimens were imported to commercial explicit FE software (Dassault Systèmes Simulia Corp. (2009)). Every side of the specimen was confined by shell plates. Loading was applied by imposing velocity on opposing plates. The velocity would correspond to the targeted strain rate in the order of 10^{-2}. The rest of the plates were constraint by imposing a linear relation for displacements of opposing faces. Boundary conditions were imposing that opposite lateral faces moved by uniform displacements, perpendicular to the faces and of equal and opposite amount. The contact settings (surface to surface contact algorithm) between the plates and foam would only allow for the specimen and plate nodes to slide tangentially and frictionless to the plates. Separation was not allowed in the normal direction.

The parent material was experimentally tested in quasi static compression and tension (Siegkas et al. (2011)). A standard J_2 plasticity model was used to model the parent material behavior.

Results and discussion Fig. 5 compares the compressive response of foam of density ρ=1625 kgm^{-2} between FE predictions using a J_2 plasticity model for the parent material and experimental data. Experimental data were obtained using a commercial screw driven loading setup in displacement control. The compressive force was measured by a resistive load cell, and the shortening of the sample was measured by a high precision and frequency laser extensometer that was used to calculate the compressive strain (described by Siegkas et al. (2011)). Voronoi tessellations were used for the generation of irregular foam geometries. Voronoi polyhedral are commonly used as shells of closed-cell high porosity foams (Zhu et al. (2000), Ma et al. (2009)). However in this study the 3D Voronoi polyhedrals were used as precursors around which the material forms open cell geometry. The method allows for statistical control of various foam features and is able to capture microstructural effects such as irregularity and texture of real foams.

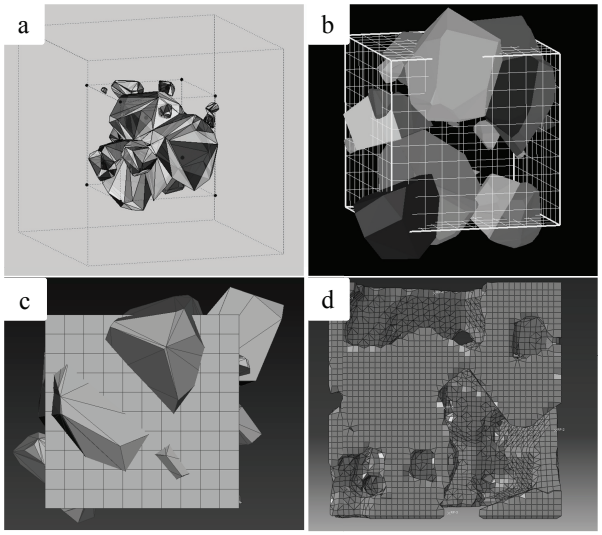

Fig. 4. (a) Voronoi polyhedrals produced in Matlab, (b) Confined polyhedrals in LS Pre-post, (c) polyhedrals and shell confinement imported in Ansa mesh generator, (d) foam geometry imported in Abaqus CAE.

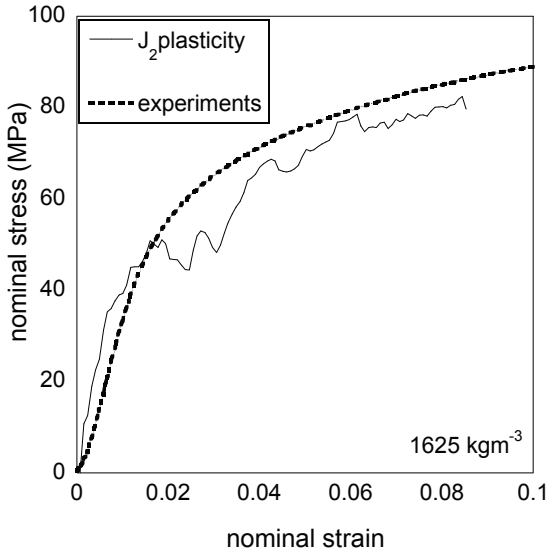

Fig. 5. Comparison of uniaxial compression experiment with FE predictions for a foam of density ρ=1625 kgm^{-2}. J_2 plasticity model was used to model the parent material.

3. **CONCLUSIONS**

The method proposed in this study for producing foam structures was able to capture geometrical characteristics of irregular foam geometries and produce specimens for FE simulations. FE predictions of compressive loading of structures were able to reproduce mechanical characteristics of Ti foams of this type and behave in good agreement with experimental data.

References

Ansa, 2007. Ansa User's Guide, Beta CAE Systems.

Borovinšek, M., Ren, Z., 2008. Computational modelling of irregular open-cell foam behaviour under impact loading. Materialwissenschaft und Werkstofftechnik 39, 114–120.

Davies, G. J., Zhen, S., 1983. Metallic foams: their production, properties and applications. Journal of Materials Science 18, 1899–1911.

Eppley, B. L., Sadove, A. M., 1990. Effects of material porosity on implant bonding strength in a craniofacial model.Journal of Craniofacial Surgery 1, 191–5.

Dassault Systèmes Simulia Corp. (2009) Abaqus Analysis User's Manual, version 6.9 Dassault Systèmes Simulia Corp., Providence, RI

Imwinkelried, T., 2007. Mechanical properties of open-pore titanium foam. Journal of Biomedical Materials Research Part A 81, 964–970.

Karageorgiou, V., Kaplan, D., 2005. Porosity of 3D biomaterial scaffolds and osteogenesis. Biomaterials, 26, 5474–5491.

Khanoki, S. A., Pasini, D. 2012. Multiscale design and multiobjective optimization of orthopedic hip implants with functionally graded cellular material. Journal of biomechanical engineering 134, 031004.

L. S. T. Corporation, 2007. LS DYNA user's manual, Volume 1, Version 971.

Li, Y., GUO, Z., HAO, J., REN, S., 2008. Porosity and mechanical properties of porous titanium fabricated by gelcasting. Rare metals 27, 282–286.

Ma, G. W., Ye, Z. Q., Shao, Z. S., 2009. Modeling loading rate effect on crushing stress of metallic cellular materials. International Journal of Impact Engineering 36, 775–782.

Mathworks, 2002. Matlab Help Files, Solution of Equations, Campridge MA.

Navarro, M., Michiardi, A., Castano, O., Planell, J. A., 2008. Biomaterials in orthopaedics. Journal of the Royal Society Interface 5, 1137–1158.

Niu, W., Bai, C., Qiu, G., Wang, Q., 2009. Processing and properties of porous titanium using space holder technique. Materials Science and Engineering: A 506, 148–151.

Oh, I. H., Nomura, N., Masahashi, N., Hanada, S., 2003. Mechanical properties of porous titanium compacts prepared by powder sintering. Scripta Materialia 49, 1197–1202.

Shen, H., Oppenheimer, S. M., Dunand, D. C., Brinson, L. C., 2006. Numerical modeling of pore size and distribution in foamed titanium. Mechanics of materials 38, 933–944.

Siegkas, P., Tagarielli, V. L., Petrinic, N., Lefebvre, L. P., 2011. The compressive response of a titanium foam at low and high strain rates. Journal of Materials Science 46, 2741–2747.

Singh, R., Lee, P. D., Lindley, T. C., Kohlhauser, C., Hellmich, C., Bram, M., Dashwood, R. J., 2010. Characterization of the deformation behavior of intermediate porosity interconnected Ti foams using micro-computed tomography and direct finite element modeling. Acta biomaterialia 6, 2342–2351.

Sitek, A., Huesman, R. H., Gullberg, G. T., 2006. Tomographic reconstruction using an adaptive tetrahedral mesh defined by a point cloud.Medical Imaging, IEEE Transactions on 25, 1172–1179.

Voronoï, G., 1908. Nouvelles applications des paramètres continus à la théorie des formes quadratiques. Deuxième mémoire. Recherches sur les parallélloèdres primitifs. Journal für die reine und angewandte Mathematik 134, 198–287.

Zhu, H. X., Hobdell, J. R., Windle, A. H., 2000. Effects of cell irregularity on the elastic properties of open-cell foams. Acta materialia 48, 4893–4900.